NeuroImage: Clinical 34 (2022) 102998

Contents lists available at ScienceDirect

NeuroImage: Clinical

journal homepage: www.elsevier.com/locate/ynicl

Quantification of infarct core signal using CT imaging in acute ischemic stroke

Uma Maria Lal-Trehan Estrada [a], Grant Meeks [b], Sergio Salazar-Marioni [b], Fabien Scalzo [e], Mudassir Farooqui [d], Juan Vivanco-Suarez [d], Santiago Ortega Gutierrez [d,1], Sunil A. Sheth [b,1], Luca Giancardo [a,c,1,*]

[a] Center for Precision Health, School of Biomedical Informatics, University of Texas Health Science Center at Houston, Houston, TX, USA
[b] McGovern Medical School, University of Texas Health Science Center at Houston, Houston, TX, USA
[c] Institute for Stroke and Cerebrovascular Diseases, University of Texas Health Science Center at Houston, Houston, TX, USA
[d] Department of Neurology, University of Iowa Hospitals and Clinics, Iowa City, IA, USA
[e] Pepperdine University, Malibu, CA, USA

ARTICLE INFO

Keywords:
Acute ischemic stroke
Infarct core
NCCT
CTA
CTA timing
Infarct core signal

ABSTRACT

In stroke care, the extent of irreversible brain injury, termed infarct core, plays a key role in determining eligibility for acute treatments, such as intravenous thrombolysis and endovascular reperfusion therapies. Many of the pivotal randomized clinical trials testing those therapies used MRI Diffusion-Weighted Imaging (DWI) or CT Perfusion (CTP) to define infarct core. Unfortunately, these modalities are not available 24/7 outside of large stroke centers. As such, there is a need for accurate infarct core determination using faster and more widely available imaging modalities including Non-Contrast CT (NCCT) and CT Angiography (CTA).

Prior studies have suggested that CTA provides improved predictions of infarct core relative to NCCT; however, this assertion has never been numerically quantified by automatic medical image computing pipelines using acquisition protocols not confounded by different scanner manufacturers, or other protocol settings such as exposure times, kilovoltage peak, or imprecision due to contrast bolus delays. In addition, single-phase CTA protocols are at present designed to optimize contrast opacification in the arterial phase. This approach works well to maximize the sensitivity to detect vessel occlusions, however, it may not be the ideal timing to enhance the ischemic infarct core signal (ICS).

In this work, we propose an image analysis pipeline on CT-based images of 88 acute ischemic stroke (AIS) patients drawn from a single dynamic acquisition protocol acquired at the acute ischemic phase. We use the first scan at the time of the dynamic acquisition as a proxy for NCCT, and the rest of the scans as a proxy for CTA scans, with bolus imaged at different brain enhancement phases. Thus, we use the terms "NCCT" and "CTA" to refer to them. This pipeline enables us to answer the questions *"Does the injection of bolus enhance the infarct core signal?"* and *"What is the ideal bolus timing to enhance the infarct core signal?"* without being influenced by aforementioned factors such as scanner model, acquisition settings, contrast bolus delay, and human reader errors. We use reference MRI DWI images acquired after successful recanalization acting as our gold standard for infarct core.

The ICS is quantified by calculating the difference in intensity distribution between the infarct core region and its symmetrical healthy counterpart on the contralateral hemisphere of the brain using a metric derived from information theory, the Kullback-Leibler divergence (KL divergence). We compare the ICS provided by NCCT and CTA and retrieve the optimal timing of CTA bolus to maximize the ICS.

In our experiments, we numerically confirm that CTAs provide greater ICS compared to NCCT. Then, we find that, on average, the ideal CTA acquisition time to maximize the ICS is not the current target of standard CTA protocols, i.e., during the peak of arterial enhancement, but a few seconds afterward (median of 3 s; 95% CI [1.5,

Abbreviations: ICS, Infarct Core Signal (difference in intensity distribution between the infarct core region and the contralateral region; OCS, Out of Core Signal (difference in intensity distribution between the affected hemisphere and the contralateral hemisphere).

* Corresponding author at: Center for Precision Health, School of Biomedical Informatics, University of Texas Health Science Center at Houston, Houston, TX, USA.
E-mail address: luca.giancardo@uth.tmc.edu (L. Giancardo).

[1] Equal contribution.

https://doi.org/10.1016/j.nicl.2022.102998
Received 22 November 2021; Received in revised form 3 March 2022; Accepted 28 March 2022
Available online 30 March 2022

3.0]). While there are other studies comparing the prediction potential of ischemic infarct core from NCCT and CTA images, to the best of our knowledge, this analysis is the first to perform a quantitative comparison of the ICS among CT based scans, with and without bolus injection, acquired using the same scanning sequence and a precise characterization of the bolus uptake, hence, reducing potential confounding factors.

1. Introduction

Stroke is the 5th leading cause of death and the 1st leading cause of disability worldwide (Virani et al., 2020) and acute ischemic stroke (AIS) accounts for 87 % of all strokes (Benjamin et al., 2017). For patients with AIS, "time is brain". The extent of irreversible injury, termed infarct core, plays a key role in determining eligibility for acute treatments in AIS, which include intravenous thrombolysis and endovascular reperfusion therapies. Specifically, patient selection for these treatments is currently based on the ischemic infarct core size solely and/or the size ratio between the penumbra, which is the affected potentially salvageable tissue, and the infarct core (Catanese et al., 2017).

In many of the randomized clinical trials of these reperfusion therapies (Berkhemer et al., 2015; Campbell et al., 2015; Goyal et al., 2016; Jovin et al., 2015; Saver et al., 2015), infarct core was determined using MRI Diffusion-Weighted Imaging (DWI) or CT Perfusion (CTP). Unfortunately, these modalities are not available 24/7 outside of large hospitals (Kim et al., 2021). As such, there is a need for accurate infarct core determinations using more widely available imaging modalities including Non-Contrast CT (NCCT) and CT Angiography (CTA). This problem has been pursued with automated machine learning approaches (Hokkinen et al., 2021; Hornung et al., 2020; Kuang et al., 2021; Lo et al., 2019; Peter et al., 2017; Qiu et al., 2020; Sheth et al., 2019; Srivatsan et al., 2019; Wu et al., 2019; Zhang et al., 2018) and visual semiquantitative inspection (NCCT / CTA-ASPECTS score) (Coutts et al., 2004; Lee et al., 2020).

Prior studies have suggested that CTA provides improved predictions of infarct core relative to NCCT; however, this assertion has never been numerically quantified on a medical image computing pipeline on comparable acquisition protocols. In addition, single-phase CTA protocols are at present designed to optimize contrast opacification in the arterial phase (ACR-ASNR-SPR, 2020). This approach is used to maximize the sensitivity to detect vessel occlusions (Almekhlafi et al., 2019), but it is unknown whether this represents the ideal timing to detect ischemic infarct core.

In this study, we propose an image analysis pipeline based on CT images, with and without contrast, that are drawn from a single dynamic acquisition protocol, and reference MRI DWI images acting as our gold standard for infarct core that were obtained shortly after. We use the first scan in time of the dynamic acquisition as a proxy for NCCT, and the rest of the scans as a proxy for CTA images; therefore, we use the terms "NCCT" and "CTA" to refer to them. We use "CT(A)" to refer to both NCCT and CTA. This pipeline enables us to quantify and compare the ischemic infarct core signal (ICS), which is the difference in intensity distribution between the infarct core region and the contralateral side, of CTAs and NCCT, and to determine the optimal timing for CTA to maximize the ICS.

In particular, we work with whole-brain CT perfusion source images (CTP-SI) obtained from a single dynamic acquisition protocol acquired at the acute ischemic phase and MRI DWI scans acquired after successful recanalization. The CTP-SI are equivalent to a NCCT followed by a sequence of low radiation CTA scans with bolus imaged at different brain enhancement phases.

Our pipeline quantifies inter-hemispheric intensity differences using the Kullback-Leibler divergence, an information-based metric, on a predetermined infarct core region of interest determined by MRI DWI. Using this quantitative measurement, we are able to quantify the amount of "information" available to estimate infarct core from our proxy NCCT or CTA and the optimal timing of CTA bolus to maximize this information metric. This is particularly important for the design of image-based machine learning algorithms aimed at predicting stroke-related outcomes. In addition, we show examples of how the Kullback-Leibler divergence between symmetrical patches of the brain can highlight inter-hemispheric brain changes even without using a predetermined area on CT(A).

In this work, we are not trying to build or evaluate segmentation approaches but rather use the pipeline developed to inform whether or not an injection of contrast bolus improves the ICS and when is the time that optimizes this improvement. These findings can support the development of automatic and manual image segmentation pipelines, regardless of the segmentation approach used.

2. Materials and methods

2.1. Data and patient cohort

The data used in this work was acquired from the University of Iowa Hospitals & Clinics, Iowa City, United States. All the data used were part of studies reviewed and approved by the Committee for the Protection of Human Subjects at The University of Iowa and The University of Texas Health Science Center at Houston (IRBs # 201,910,789 and HSC-MS-20–1266). Patient consent was waived because of the retrospective nature of the study cohort. Patients were included in this study if they were diagnosed with AIS due to proximal anterior circulation large vessel occlusion, underwent imaging with a whole-brain dynamic acquisition protocol (CTP-SI), underwent endovascular therapy that resulted in successful reperfusion within 97 [78 – 122] minutes of the acquisition, and had MRI DWI imaging within 24 h post-procedure. Since in our cohort, we select only subjects that had successful endovascular stroke therapy, we do not expect the infarct core to have changed significantly from the reperfusion therapy until the MRI DWI acquisition (Krongold et al., 2014).

The dynamic contrast acquisition was performed with 40 mL of nonionic iodinated contrast (Isovue-370) followed by 50 mL of saline. The acquisition protocol included a rapid sequential scanning, with 4 scans each 3 s apart followed by 15 scans 1.5 s apart and another 9 scans 3 s apart, totaling 28 scans over approximately 60 s (Limaye et al., 2019). For the purposes of this study, the NCCT image was retrieved from the first acquisition of the sequence. The subsequent images were considered dynamic CTA images.

Both MRI scans and CTP-SI were acquired from the same manufacturer, Siemens. Our dataset contained a total of 88 subjects. In Table 1, we summarize the main clinical variables of our cohort: patient age, patient sex, the ischemic infarct core volume (with a median of 31 mL and an interquartile range of [16 mL, 60 mL]), the affected artery by the stroke, which can be the middle cerebral artery (MCA) or the internal carotid artery (ICA), the affected artery segment (segments M1, M2 or M3 in the case of affected MCA, and segments T and cervical in the case of affected ICA) and the thrombolysis in cerebral infarction (TICI) score, which for all cases is equal or greater than "Grade 2B", that is to say, all cases had a successful recanalization.

In Table 2, the median and the interquartile range of the time difference in hours between the acquisition of the CTP-SI and the last known well (LWK) and the time difference between the MRI acquisition and the reperfusion therapy are reported.

The infarct core was manually segmented from the MRI DWI sequences acquired within 24 h after successful recanalization. Segmented volumes were created using 3D Slicer (Fedorov et al., 2012) by a trained

Table 1
Dataset description: patient age, patient sex (F: female), ischemic core volume, affected artery (ICA: internal carotid artery; MCA: middle cerebral artery), affected segment, and TICI (thrombolysis in cerebral infarction) score. In bold, is the most frequent category for each variable. The ischemic infarct core median is 31 mL. Note that all patients had a successful recanalization (TICI score ≥ Grade 2B).

VARIABLES		Number (%) of cases (Total of 88 patients)
AGE	< 20	0 (0.00 %)
	>= 20 < 40	4 (4.55 %)
	>= 40 < 60	18 (20.45 %)
	>= 60 < 80	**44 (50.00 %)**
	>= 80	22 (25.00 %)
SEX	F	**46 (52.28 %)**
ISCHEMIC INFARCT CORE VOLUME ONMRI DWI SEGMENTATIONS (mL)	< 30	**44 (50.00 %)**
	>= 30 < 50	16 (18.18 %)
	>= 50 < 70	9 (10.23 %)
	>= 70	19 (21.59 %)
AFFECTED ARTERY	ICA	15 (17.05 %)
	MCA	**73 (82.95 %)**
AFFECTED SEGMENT	ICA	1 (1.14 %)
	CERVICAL	
	ICA T	12 (13.64 %)
	MCA M1	**53 (60.23 %)**
	MCA M2	20 (22.73 %)
	MCA M3	2 (2.27 %)
TICI SCORE	GRADE 2B	**44 (50.00 %)**
	GRADE 2C	10 (11.36 %)
	GRADE 3	34 (38.64 %)

Table 2
Time difference between the CTP-SI acquisition and the last known well time (CTP-SI TIME – LKW TIME) and time difference between the MRI acquisition and the reperfusion therapy (MRI TIME – REPERFUSION TIME) measured in hours (h). The median CTP-SI acquisition time was approximately 4 h after the LKW. The median MRI acquisition time was approximately 19 h after the reperfusion time.

Time difference	TIME (h)
CTP-SI TIME – LKW TIME	4.18 [3.12 – 8.01]
MRI TIME – REPERFUSION TIME	18.93 [8.13 – 22.95]

cerebrovascular researcher and vetted by an expert Vascular Neurologist (SSM, SS).

2.2. Image Pre-processing

Image registration was performed to align the CTP-SI and the MRI DWI images to a common space. For all affine matrices estimation, we used Elastix (Klein et al., 2010) to identify rigid affine registrations using a multi-resolution strategy with a normalized correlation as a metric for the optimization process. In each patient, the MRI DWI scan was registered to the CTP-SI space obtaining the affine matrix A_{DWI_CTP}. Since the CTP-SI consists of a 4D volume with multiple scans as a function of time, to obtain a target image template to register the MRI DWI scan to the CTP-SI space, the CTP-SI was converted to a 3D volume by computing the median voxel across time. In addition, it was clipped to the range [0, 95] Hounsfield Units (HU) and smoothed using a Gaussian filter. We refer to this 3D volume as CTP-SI_{med}. Then, the segmented infarct core was aligned to the patient CTP-SI space by applying A_{DWI_CTP}. CTP-SI_{med} is uniquely used as a template for segmented infarct core registration; further processing uses the raw CTP-SI without any time or space filtering.

After the intra-patient alignment phase, all images were registered to a custom standardized CTA template in the Montreal Neurological Institute (MNI) space referred to as CTA_{MNI}. This template had a resolution of 182 × 218 × 182 and 1 × 1 × 1 mm voxel size. For each patient, in order to have a 3D moving image for registration in the CTP-SI space, a template named CTP-$SI_{med2MNI}$ was computed, which differs from the previous CTP-SI_{med} used for the intra-patient alignment in the clipping part, since only values lower than 0 were clipped to 0. This CTP-$SI_{med2MNI}$ was registered to CTA_{MNI} obtaining the affine matrix A_{CTP_MNI}. Then, A_{DWI_CTP} and A_{CTP_MNI} were combined to transform all the CTP-SI, the MRI DWI, and the manual infarct core segmentation to the CTA_{MNI} space. After these automatic transformation processes, registration results were examined visually, and registration corrections were made manually if considered necessary using 3D Slicer software (Fedorov et al., 2012). Finally, we corrected for any motion artifacts on the CTP-SI, by co-registering the source images, that is, by registering all time-frames to the CTP-SI_{med} template.

2.3. Measurements

For each patient, three enhancement phases were identified based on the arterial/venous input functions: the early arterial phase, the mid arterial phase, and the delayed venous phase. We refer to the CTP-SI scans corresponding to these 3-time points as early arterial CTA, mid arterial CTA, and delayed venous CTA, respectively. In addition, we selected the first time point of the CTP-SI when the contrast bolus was not injected and considered it as a NCCT. Fig. 1 shows an example of the data of one patient (axial slices of 4 CTP-SI at different time points).

The ICS was quantitively measured by calculating the difference in intensity distribution between the infarct core region and the corresponding non-infarcted region in the opposite hemisphere (regions visually represented in Fig. 2). Specifically, the intensity probability density function was estimated using a Gaussian kernel density estimator, and the Kullback-Leibler divergence (KL) between them was computed (see Fig. 2). We believe that the KL divergence is an excellent unbiased metric to measure the additional visual information given by the non-infarcted region compared to the infarct core region as it was specifically designed to estimate the information gain between two distributions and it has a clear statistical interpretation, i.e., the amount of information lost when the infarct core area is used to approximate the healthy contralateral region. For completeness, we also tested two other metrics, the Jensen-Shannon distance (JS), which is the symmetric version of KL, and the standard Euclidean distance (ED).

Considering two intensity probability density functions, P1 and P2 (Fig. 2), corresponding to the contralateral region and the infarct core region, respectively, and using an intensity range between 0 HU and 400 HU, which theoretically covers all possible intensities that there can be in the brain tissue (without skull) in a contrast-enhanced CT scan, the 3 metrics used to compute the ICS are the following:

- *Kullback-Leibler divergence (KL)*

$$KL\ (P1||P2) = \sum_{x \in X} P1(x) log\left(\frac{P1(x)}{P2(x)}\right) \quad (1)$$

where x is the intensity value and X goes from 0 to 400 HU.

- *Jensen-Shannon distance (JS)*

$$JS\ (P1||P2) = \frac{1}{2} KL\ (P1||M) + \frac{1}{2}\ KL\ (P2||M) \quad (2)$$

where KL is the Kullback-Leibler divergence and M is $\frac{1}{2}$(P1 +P2).

- *Euclidean distance (ED)*

$$ED\ (P1||P2) = \sqrt{\sum_{x \in X} (P1(x) - P2(x))^2} \quad (3)$$

where x is the intensity value and X goes from 0 to 400 HU.

It should be noticed that JS and ED are symmetric, while KL is not symmetric, that is to say, KL(P1||P2) ≠ KL(P2||P1), as such it is not

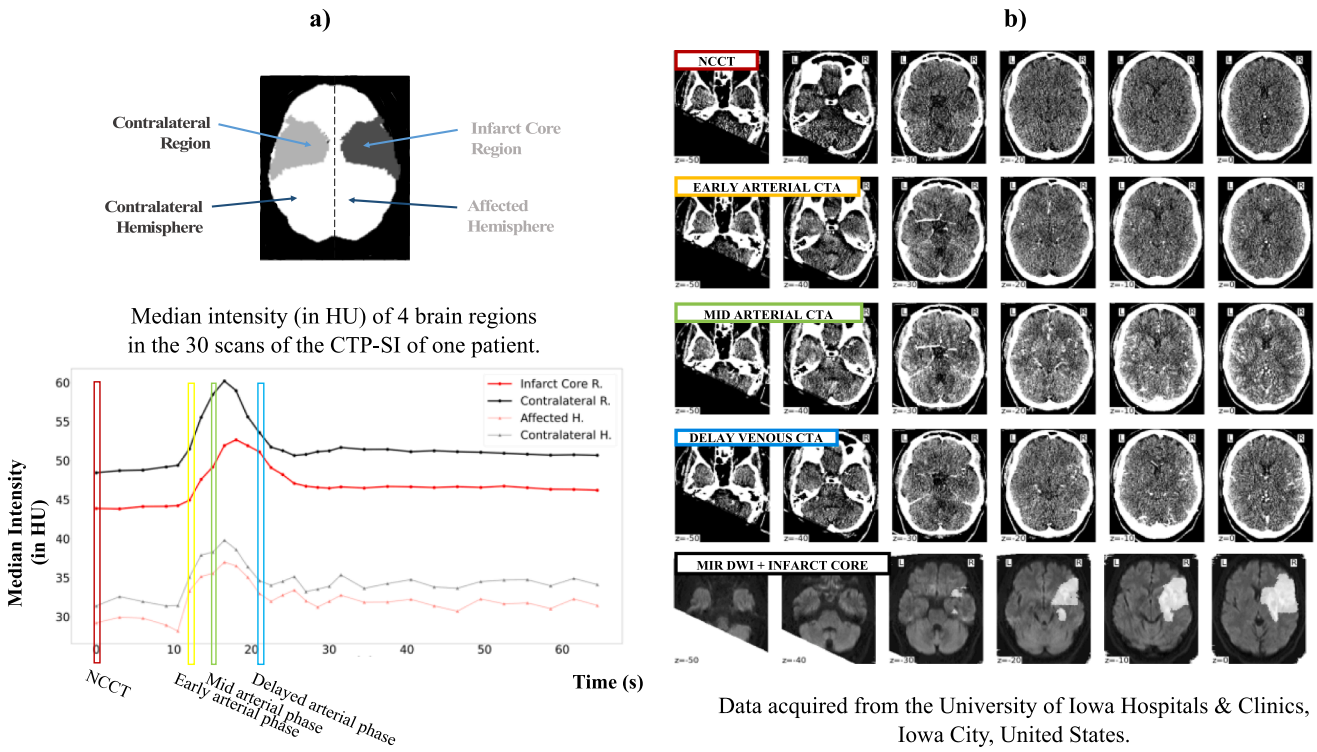

Fig. 1. a) Diagram of the brain showing 4 different regions (infarct core region, contralateral region, affected hemisphere, and contralateral hemisphere) and median intensity in Hounsfield Units (HU) of those 4 regions of the brain for each time point of the CTP-SI of one patient of the dataset. Four different time points are indicated, the first time point in red (equivalent to a NCCT) and the time points corresponding to the early arterial phase (in yellow), mid arterial phase (in green), and delayed venous phase (in blue). NCCT: non-contrast CT. b) For the same patient, axial slices of the NCCT (1st row), early arterial CTA (2nd row), mid arterial CTA (3rd row), delayed venous CTA (4th row), and MRI DWI and manual infarct core segmentation overlayed in white (4th row). Note how the vessel's enhancement changes in the CTP-SI at different time points (from no enhancement in the NCCT to increasing enhancement in the other CTAs) and the difficulty to visually distinguish the infarct core region from these low radiation CTAs. (For interpretation of the references to colour in this figure legend, the reader is referred to the web version of this article.)

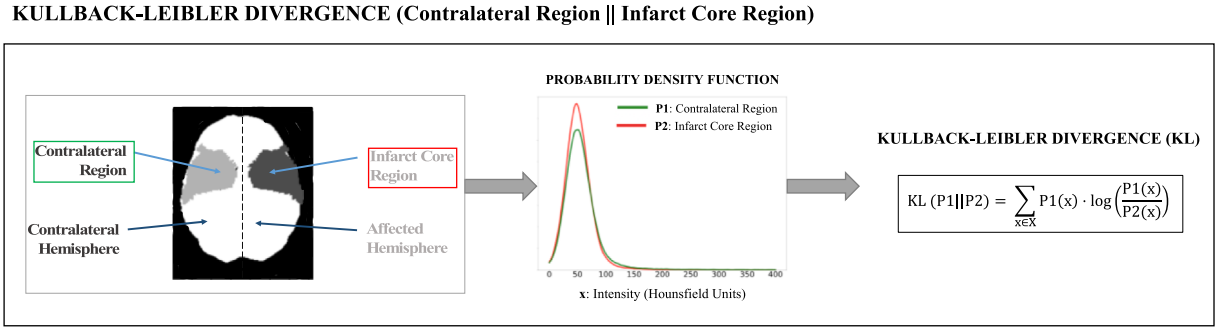

Fig. 2. Quantification of ICS using the KL divergence. First, the intensity probability distributions are estimated for these two regions. Then, the KL divergence is computed between the two probability distributions as in the formula.

technically a difference "metric". Note we chose KL (contralateral region || infarct core region) as this allows us to measure the information loss when the infarct core region is used to approximate the healthy contralateral region. As the infarcted region is expected to show a texture that is typically darker and with less contrast, this will result in a higher value for the ICS.

The three measurements (KL, JS, and ED) were computed for the NCCT and all-time points of the CTP-SI during the injection of the contrast agent. The time point providing the greatest value was defined as the **ideal time**. The scan of the CTP-SI corresponding to the ideal time was referred to as **ideal CT(A)**. The time difference between the ideal time and the mid arterial phase time was calculated for each patient. The median of this time difference across the cohort is referred in what follows to as the **group-level ideal time**. The group-level ideal time is estimated using bootstrap of 90% of the dataset running 1000 iterations. The mid arterial phase time was chosen as a reference since it is the target of current CTA protocols. The scan of the CTP-SI corresponding to the group-level ideal was referred to as group-level ideal CT(A).

The values of the KL, JS, and ED were statistically compared using Wilcoxon signed-rank test between all the possible pairs from the following 6 scans:

- NCCT: first CTP-SI scan.
- Early arterial CTA: CTP-SI scan corresponding to the early arterial phase.
- Mid arterial CTA: CTP-SI scan corresponding to the mid arterial phase.

- Delayed venous CTA: CTP-SI scan corresponding to the delayed venous phase.
- Ideal CT(A): CTP-SI scan providing the highest difference between the infarct core region and the contralateral region (specific to the metric used to compute this difference (KL, JS, ED)).
- Group-level ideal CT(A): CTP-SI scan at the group-level ideal time.

The primary outcomes for this study were the determination of the ideal time for CTA acquisition across the cohort and its relative difference with respect to the mid arterial phase ("group-level ideal time"). These variables as well as the statistical analyses, apart from being computed from all the cohort, were also performed for 2 groups of patients based on the infarct core volume: group 1 (<30 mL) with 44 patients and group 2 (>=30 mL) with 44 patients.

Of note, a sensitivity analysis was performed in which patients with intracerebral hemorrhage on MRI DWI imaging were excluded, as the true boundaries of the infarct core volume can be uncertain in this population.

2.4. Kullback-Leibler divergence brain map

To qualitatively evaluate the ability of KL to detect areas of hypoperfusion, KL brain maps were created. KL was calculated between symmetrical 3D patches of the brain scans (a patch in one brain hemisphere and its symmetrical patch on the contralateral hemisphere). Patches of 21 × 21 × 21 voxels and a stride of 2 × 2 × 12 were used. Only patches fully contained in the brain (inside the skull) were considered. The resulting brain KL values for each scan are referred to as KL brain maps. For each patient, KL brain maps were obtained for the 5 first scans listed in section *2.3 Measurements* for the statistical comparison with the aim of qualitatively (visually) examining the ability of KL for detecting the infarct core at different enhancement phases of the brain vessels.

3. Results

3.1. Ideal time based on the KL divergence

Fig. 3 shows the percentage of ideal CT(A)s, using the KL divergence, grouped into 7-time levels: (1) Before the early arterial phase; (2) at the early arterial phase (yellow point); (3) between the early arterial phase and the mid arterial phase; (4) at the mid arterial phase (green point); (5) between the mid arterial phase and the delayed venous phase (in red); (6) at the delayed venous phase (blue point); (7) after the delayed venous phase. In other words, we computed the percentage of patients that have a scan at a given time level providing the highest ICS (highest KL between the contralateral region and the infarct core region). Note that the time attenuation curve represents an ideal arterial input function.

The majority of ideal CT(A)s (~70%) are the ones corresponding to a CTA acquisition between mid arterial and delayed venous phases (time level (5)). Only 9% correspond to a standard acquisition at the mid arterial phase (time level (4)), and 1.1% correspond to a NCCT acquisition (time level (1)).

The ideal CT(A) has a median time offset of + 3 s on 1000 bootstrap replicates using 90% of the data with replacement (95% CI [1.5, 3.0] seconds) from the mid arterial phase, when using KL to estimate the ICS. Using ED, the group-level ideal time is median of 3 s (95% CI [3, 4.5] seconds), and using JS, the group-level ideal time is median of 3 s (95% CI [3, 3] seconds). When grouping the patients according to their infarct core volume, similar values of group-level ideal time are obtained (see Appendix, Table A1).

Similar findings are obtained when excluding the subjects with hemorrhagic transformations (see Appendix, Fig. A1, Table A2).

3.2. KL (contralateral region || infarct core region) statistical comparison

The distribution of the KL values for each of the 6 compared scans (NCCT, early arterial CTA, mid arterial CTA, delayed venous CTA, ideal CT(A), and group-level ideal CT(A)) are shown in Fig. 4.

Pairwise ICS numerical comparisons, including statistical significance are available in Table 3. Based on the KL metric, a CTA acquired at the mid arterial phase provides a significantly greater ICS compared to a NCCT. The ICS in the ideal CT(A) and in the group-level ideal CT(A) is significantly greater than the one provided by a NCCT and by any of the other 3 CTAs analyzed, including the mid arterial CTA. There is no significant difference in the ICS between a mid arterial CTA and a delayed venous CTA.

Also, we compared the infarct core signal (ICS) with the out-of-core signal (OCS), i.e., the brain area not part of the stroke core (Fig. 4). This way, we allowed each subject to be their own control. The OCS is created following a similar method as the ICS is but it uses brain areas outside

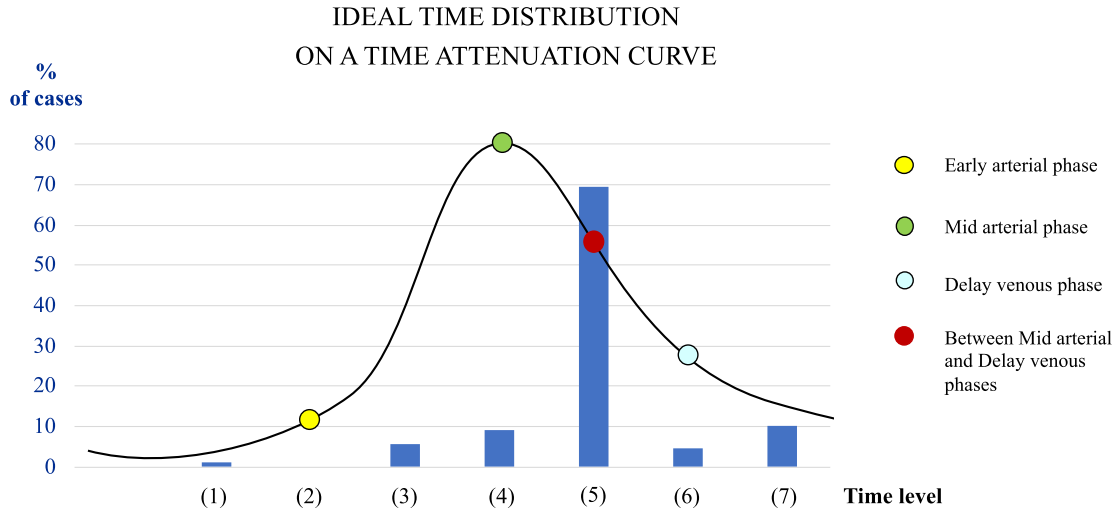

Fig. 3. Percentage of patients providing the highest ICS at 7 different time levels: (1) before the early arterial phase (1.1 %), (2) at the early arterial phase (0 %), (3) between the early and the mid arterial phases (5.7 %), (4) at the mid arterial phase (9.1 %), (5) between the mid and the delayed venous phases (69.3 %), (6) at the delayed venous phase (4.5 %) (7) and after the delayed venous phase (10.2 %). The highest ICS corresponds to the highest Kullback-Leibler divergence between the contralateral region and the infarct core region and for most cases (69.3 %) it is provided by a CTA scan acquired between the mid arterial phase and the delayed venous phase.

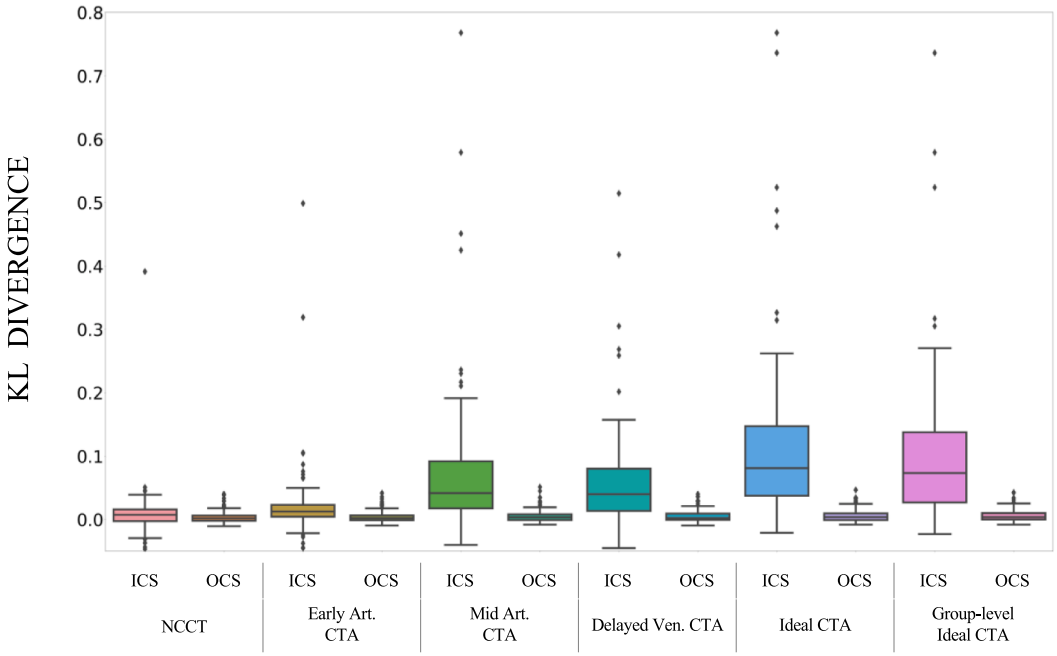

Fig. 4. Boxplots of ICS and OCS for 6 different scans (NCCT; Early arterial CTA; Mid arterial CTA; Delayed venous CTA; Ideal CT(A); group-level Ideal CT(A)) representing the distribution over the 88 patients of the Kullback-Leibler divergence between the contralateral region and the infarct core region (ICS) and between hemispheres (OCS). Ideal CT(A): time point providing the highest Kullback-Leibler divergence between the contralateral region and the infarct core region, specific for each patient. Group-level Ideal CT(A): CTA at 3 s after the mid arterial phase. Pairwise ICS numerical comparisons, including statistical significance are available in Table 3.

the infarct core. We found that the ICS is significantly higher than the OCS in all scans (NCCT, early arterial CTA, mid arterial CTA, delayed venous CTA, and ideal CT(A)) regardless of the distance metric used (see "Additional Figures / Tables" in the Appendix).

The distribution of the ED values and JS values for each of the 6 compared scans (NCCT, early arterial CTA, mid arterial CTA, delayed venous CTA, ideal CT(A), and group-level ideal CT(A)) are included in the Appendix (see Figs. A2, A3). The significance of the difference of ICS with respect to the mid arterial CTA and the group-level ideal CT(A) for different groups of patients using KL, ED, and JS to compute ICS can be seen in the Appendix (see Table A3).

3.3. Metrics comparison (ED, KL, JS)

The median value and interquartile range of the ICS based on the ED, the KL, and the JS calculated from 6 different scans can be seen in Table 3.

For all 3 metrics, the ICS (estimated by the difference in intensity between the contralateral region and the infarct core region) provided by the NCCT and the early arterial CTA is significantly lower than the one provided by the mid arterial CTA. In addition, the group-level ideal CT(A) shows a higher ICS compared to the early arterial, mid arterial, and delayed venous CTAs and the NCCT. It is worth noticing that there is no significant difference between the ICS provided by the delayed venous CTAs and the ICS provided by the mid arterial CTAs.

Equivalent results are obtained for the dataset excluding the patients with intracerebral hemorrhage on MRI DWI (see Table A4 in the Appendix).

3.4. Kullback-Leibler divergence brain map

Axial slices of the KL brain maps for 5 scans of 1 patient of the dataset and their corresponding scan axial slices along with the infarct core contour overlayed on top can be seen in Fig. 5. For this patient, the ideal CT(A) corresponds to a time point between the mid arterial phase and the delayed venous phase, as in the majority of patients (Fig. 3).

As it can be observed in Fig. 5(b), these brain maps show a much clearer visualization for estimating the infarct core as opposed to the original images shown in Fig. 5(a).

The KL brain maps from the NCCT and the early arterial CTA are more or less homogenous. Some areas not corresponding to the infarct core are enhanced. However, slightly higher intensities in the infarct core region can be seen compared to the contralateral region. The brain maps corresponding to the NCCT, and the early arterial CTA are visually very different from the brain maps corresponding to the mid arterial CTA, the ideal CT(A), and the delayed venous CTA. These 3 latter CTAs appear to show a greater ICS since KL hyperintensities shown in these KL brain maps correspond mainly to the infarct core region.

4. Discussion

Currently, the size of the infarct core, key in determining eligibility for acute treatments in AIS, is estimated using advanced imaging such as MRI and CT perfusion (CTP). Since these imaging modalities are not available 24/7 outside of large hospitals, there is a pressing need to use more widely available imaging modalities including non-contrast CT (NCCT) and CT angiography (CTA) to calculate the infarct core size.

Current single-phase CTA protocols are designed to optimize contrast opacification in the arterial phase, that is, they aim to scan the peak of

Table 3
Median and interquartile range of the ICS measured using 3 metrics (Euclidean distance, Kullback-Leibler divergence, and Jensen-Shannon distance), for 6 scan types (non-contrast CT, Early arterial CTA, Mid arterial CTA, Delayed venous CTA, Ideal CT(A), and group-level Ideal CT(A)). Higher values of the metrics correspond to higher ICS. The Ideal CT(A) is different for each metric; it corresponds to the CTA providing the highest value of the metric. The group-level Ideal CT(A) is the scan acquired at the group-level ideal time, that is, 3 s after the mid arterial phase. The distribution of the metric values for each CTA is compared to the metric values obtained for the Mid arterial CTA and the group-level Ideal CT(A). The significance of the difference is shown using the following notation: "-": equal distributions, no comparison performed; "ns" (non-significant): 5E-02 < p <= 1; "*": 1E-02 < p <= 5E-02; "**": 1E-03 < p <= 1E-02; "***": p <= 1E-03; where p is the p-value obtained in the statistical test.

	Metric used to compute ICS					
	EUCLIDEAN DISTANCE (ED)		**KULLBACK-LEIBLER DIVERGENCE (KL)**		**JENSEN-SHANNON DISTANCE (JS)**	
	Median [interquartile range]	Difference of medians and Statistical significance of Difference w.r.t Mid Arterial Phase/Difference w.r.t Group-level Ideal Phase	**Median [interquartile range]**	Difference of medians and Statistical significance of Difference w.r.t Mid Arterial Phase/Difference w.r.t Group-level Ideal Phase	**Median [interquartile range]**	Difference of medians and Statistical significance of Difference w.r.t Mid Arterial Phase/Difference w.r.t Group-level Ideal Phase
NCCT	0.010 [0.007 – 0.014]	(-0.011) *** / (-0.017) **	0.008 [-0.003 – 0.016]	(-0.034) *** / (-0.066) *** / ***	0.051 [0.039 – 0.066]	(-0.050) *** / (-0.084) *** / ***
EARLY ARTERIAL CTA	0.012 [0.007 – 0.017]	(-0.009) *** / (-0.015) ***	0.013 [0.004– 0.023]	(-0.029) *** / (-0.061) *** / ***	0.063 [0.044– 0.086]	(-0.036) *** / (-0.071) *** / ***
MID ARTERIAL CTA	0.021 [0.012 – 0.026]	- / (-0.006) ***	0.042 [0.018 – 0.092]	- / (-0.032) ***	0.100 [0.069 – 0.139]	- / (-0.035) ***
DELAYED VENOUS CTA	0.021 [0.012 – 0.029]	(0.000) ns / (-0.005) ***	0.040 [0.014 – 0.080]	(-0.002) ns / (-0.033) ***	0.107 [0.062 – 0.136]	(0.007) ns / (-0.027) ***
IDEAL CT(A)	0.027 [0.019 – 0.033]	(0.006) *** / (0.000) ***	0.081 [0.038 – 0.147]	(0.039) *** / (0.008) *** / ***	0.141 [0.105 – 0.170]	(0.041) *** / (0.007) *** / ***
GROUP-LEVEL IDEAL CT(A)	0.027 [0.016 –0.032]	(0.005) *** / -	0.073 [0.027 – 0.138]	(0.032) *** / -	0.134 [0.084 – 0.164]	(0.035) *** / -

arterial enhancement, also referred to as mid arterial phase, this allows them to optimize the detection of occlusions. Whether this is the best CTA acquisition time to detect the infarct core and whether it is better than a NCCT is unclear. For this reason, in this work, we have developed a medical image computing pipeline to quantify and compare the infarct core signal (ICS), which is the difference in intensity distribution between the infarcted tissue and the contralateral side, from proxy NCCT and CTA images. It should be remarked that this comparison uses images that have been drawn from a single dynamic acquisition protocol (CTP-SI), using the same scanner and protocol for each patient. This allowed to limit the amount of potential confounders significantly. In particular, the CTP-SI can be seen as a NCCT (first scan of the CTP-SI) followed by a sequence of low-radiation CTA scans.

Standard clinical NCCTs and CTAs not derived from a single CTP-SI acquisition can have very different X-ray exposure times and the Kilovoltage Peak (KVp) parameters, as such they can be significant confounders in a head-to-head comparison of NCCT and CTA. While we are using scans drawn from a single dynamic acquisition protocol, which is not how NCCT or CTA images are typically acquired clinically, we are able to perform a comparative analysis without including these confounding factors that would influence the image contrast. In addition, the comparison we propose avoids the influence of factors such as scanner model, protocols, and human reader bias/experience, which would happen in the case of comparing NCCT-ASPECTS to CTA-ASPECTS. While there are other studies comparing NCCT and CTA for infarct core determination, to the best of our knowledge, this is the first analysis that compares CT acquisitions with and without contrast acquired under the same acquisition protocol and without using a human reader.

With this analysis, we show that CTAs provide higher ICS compared to NCCTs and that a CTA scan acquired approximately 3 s after the mid arterial phase maximizes the ICS. Therefore, we hypothesize that current CTA protocols targeting the mid arterial phase are not the most appropriate for detecting the ischemic infarct core, but the best timing to scan corresponds to approximately 3 s after the current target time point.

The results we show in this work are based on the Kullback-Leibler divergence (KL), metric that is used to compute the difference in intensity distribution between the ischemic infarct core region and the contralateral region. The same difference has been computed using the Euclidean distance and the Jensen-Shannon distance. The overall conclusion obtained by any of these 3 metrics is equivalent. Using all 3 metrics, a standard CTA provides greater ICS than a NCCT, and the ideal phase of acquisition of the CTA to maximize the ICS is between the mid arterial and the delayed venous phases (median of 3 s after the mid arterial phase). However, the KL divergence showed a difference between the NCCT and the ideal CT(A) much larger than what can be detected with the ED, and compared to the JS it enables to distinguish the hemisphere affected by the infarct. In addition, the theory behind the KL allows a clear interpretation of its values as it represents the amount of information lost when the infarct core region is used to approximate the healthy contralateral region. By computing the KL between symmetrical 3D patches of the brain scans (without using a priori information of the core location), we can obtain KL brain maps whose hyperintensities appear to be particularly pronounced in the infarct core region.

It should be remarked that the circulation timing is a patient-specific variable. The enhancement change in a certain period of time is not the same for all patients. In this work, we have not accounted for the causes

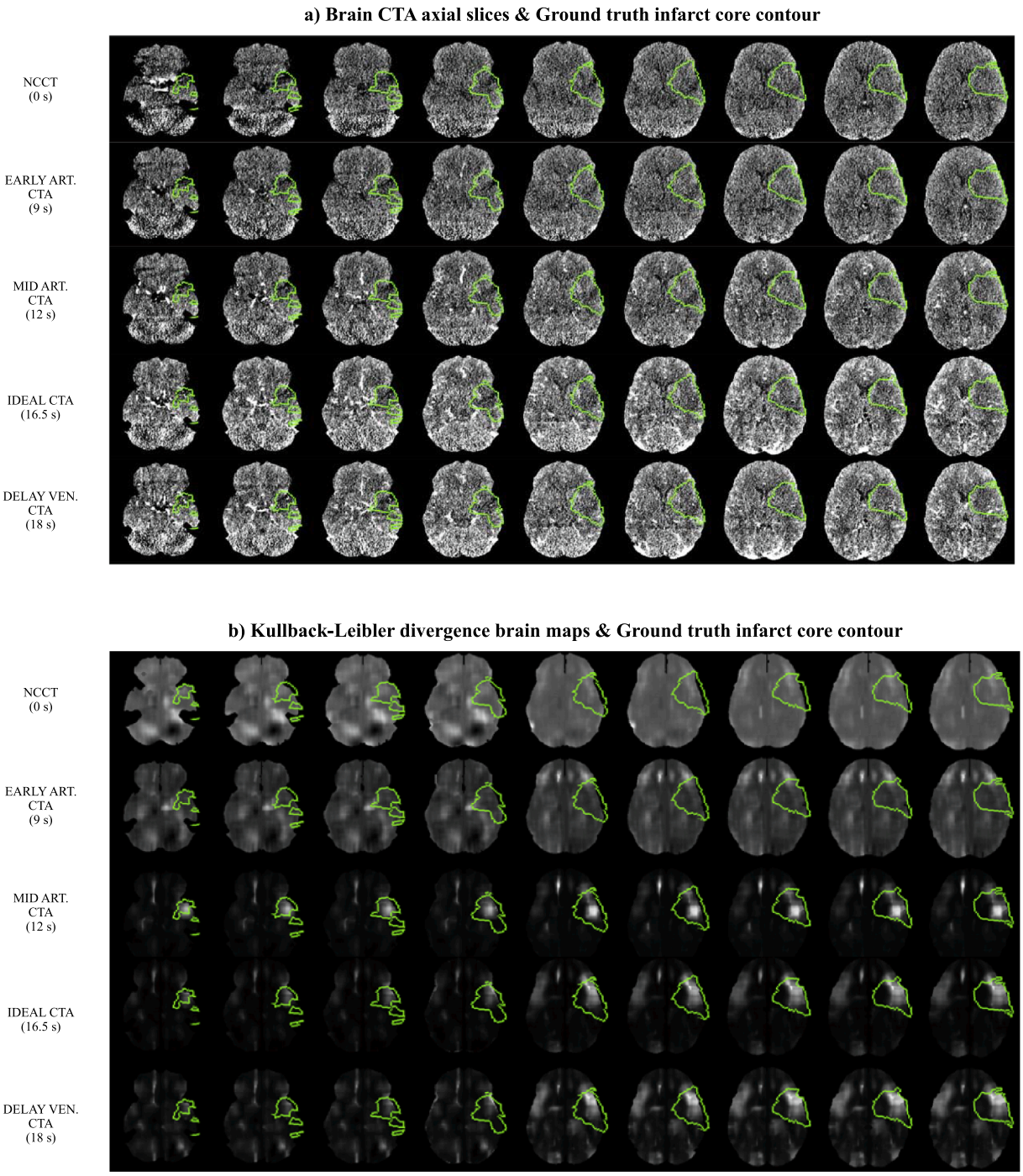

Fig. 5. a) Axial slices of 5 brain scans of 1 patient of the dataset (5 rows for each of the 5 different scans) and corresponding overlayed ground truth infarct core contour in green. B) For the same patient as in a), axial slices of the Kullback-Leibler divergence (KL) brain maps were obtained from the same 5 scans and corresponding overlayed ground truth infarct core contour in green. Scans: non-contrast CT (NCCT), Early arterial CTA, Mid arterial CTA, Ideal CT(A), Delayed venous CTA. The ideal CT(A) corresponds to the CT scan at which the KL between the contralateral region and the infarct core region is higher. For each CTA, the scan starting time after contrast injection is indicated in parenthesis. Note the ability of KL to detect the infarct core region from the Ideal CT(A) (4th row in b), detecting more voxels from the infarct core region than in the case of the mid arterial CTA and leading to fewer false positives than in the case of the delayed venous CTA. (For interpretation of the references to colour in this figure legend, the reader is referred to the web version of this article.)

that can affect enhancement time. Our results show that the ideal CT(A) time for measuring the infarct core is approximately 3 s after the mid arterial phase. These 3 s correspond to the median of the ideal CT(A) time over 1000 bootstrap replicates using 90% of the data with replacement. Therefore, it is an approximation that does not consider the differences in the circulation timing. We looked at two possible predictors of the ideal time: Last known well time and occlusion location, and while we see some trends, the results are not conclusive. Analysis of these predictors can be found in the Appendix. Additional reasons for this variability could also be due to patient-specific factors like cardiac output or stenoses in vascular systems.

In our experiments, we considered only single-phase acquisitions to adjudicate to measure ICS, however, multiphase CTA-based approaches have been successfully implemented, for example by McDougall et al.

(2020) and Menon et al. (2015), using 3 subsequent CTA acquisitions starting at the mid arterial phase.

This work has some limitations. First, 9 out of the 88 patients in our dataset showed various degrees of hemorrhagic transformation on the MRI DWI acquired after the reperfusion. Since the true boundaries of the infarct core volume can be uncertain in this population, the same analysis performed with the whole dataset has been performed as well with the dataset excluding these 9 cases. However, no significant differences have been observed in the results. Second, the infarct core signal has been estimated by considering only the voxels of the infarct core region and the contralateral region. The intensities of the rest of the brain have not been taken into account in the ICS comparison. Third, our evaluation of the KL brain maps is uniquely qualitative with the purpose of providing a visual example for the readers; a thorough evaluation of its use as an infarct core segmentation tool and its use as an additional feature for machine learning segmentation algorithms is left for further work.

5. Conclusions

We propose an image analysis pipeline based on proxy NCCT and CTA images that are drawn from a single dynamic acquisition protocol to answer two main questions in the context of acute ischemic stroke: "what is the optimal timing for CTA that maximizes the ICS?" and "does CTA provide higher ICS than NCCT?". We numerically and visually confirm that CTAs provide greater ICS compared to NCCT. Then, we find that the ideal CT(A) acquisition time to maximize the ICS is not the current target of CTA protocols, i.e., during the peak of arterial enhancement, but approximately 3 s later. Further investigation will include the comparison of the results of an automatic infarct core segmentation algorithm on CTA scans at different time points and a quantitative evaluation of KL brain maps.

6. Data and code availability statement

Data and code are available under reasonable requests. Data requests should be directed to Santiago Ortega Gutierrez.

CRediT authorship contribution statement

Uma Maria Lal-Trehan Estrada: Methodology, Software, Visualization, Writing – original draft, Writing – review & editing. **Grant Meeks:** Data curation, Writing – review & editing. **Sergio Salazar-Marioni:** Data curation, Writing – review & editing. **Fabien Scalzo:** Writing – review & editing. **Mudassir Farooqui:** Data curation, Writing – review & editing. **Juan Vivanco-Suarez:** Data curation, Writing – review & editing. **Santiago Ortega Gutierrez:** Conceptualization, Supervision, Resources, Writing – review & editing. **Sunil A. Sheth:** Conceptualization, Supervision, Writing – review & editing, Funding acquisition. **Luca Giancardo:** Conceptualization, Supervision, Methodology, Software, Writing – review & editing, Funding acquisition.

Declaration of Competing Interest

The authors declare that they have no known competing financial interests or personal relationships that could have appeared to influence the work reported in this paper.

Acknowledgments

This work has been supported by NIH grant R01NS121154. LG is supported in part by the Translational Research Institute through NASA Cooperative Agreement NNX16AO69A, NIH grants UL1TR003167, and a Cancer Prevention and Research Institute of Texas grant (RP 170668).

Appendix A. Supplementary data

Supplementary data to this article can be found online at https://doi.org/10.1016/j.nicl.2022.102998.

References

Almekhlafi, M.A., Kunz, W.G., Menon, B.K., McTaggart, R.A., Jayaraman, M.V., Baxter, B.W., Heck, D., Frei, D., Derdeyn, C.P., Takagi, T., Aamodt, A.H., Fragata, I. M.R., Hill, M.D., Demchuk, A.M., Goyal, M., 2019. Imaging of Patients with Suspected Large-Vessel Occlusion at Primary Stroke Centers: Available Modalities and a Suggested Approach. AJNR Am. J. Neuroradiol. 40, 396–400. https://doi.org/10.3174/ajnr.A5971.

Benjamin, E.J., Blaha, M.J., Chiuve, S.E., Cushman, M., Das, S.R., Deo, R., de Ferranti, S. D., Floyd, J., Fornage, M., Gillespie, C., Isasi, C.R., Jiménez, M.C., Jordan, L.C., Judd, S.E., Lackland, D., Lichtman, J.H., Lisabeth, L., Liu, S., Longenecker, C.T., Mackey, R.H., Matsushita, K., Mozaffarian, D., Mussolino, M.E., Nasir, K., Neumar, R.W., Palaniappan, L., Pandey, D.K., Thiagarajan, R.R., Reeves, M.J., Ritchey, M., Rodriguez, C.J., Roth, G.A., Rosamond, W.D., Sasson, C., Towfighi, A., Tsao, C.W., Turner, M.B., Virani, S.S., Voeks, J.H., Willey, J.Z., Wilkins, J.T., Wu, J. H.Y., Alger, H.M., Wong, S.S., Muntner, P., 2017. Heart Disease and Stroke Statistics—2017 Update. Circulation 135, e146–e603. https://doi.org/10.1161/CIR.0000000000000485.

Berkhemer, O.A., Fransen, P.S.S., Beumer, D., van den Berg, L.A., Lingsma, H.F., Yoo, A. J., Schonewille, W.J., Vos, J.A., Nederkoorn, P.J., Wermer, M.J.H., van Walderveen, M.A.A., Staals, J., Hofmeijer, J., van Oostayen, J.A., Lycklama à Nijeholt, G.J., Boiten, J., Brouwer, P.A., Emmer, B.J., de Bruijn, S.F., van Dijk, L.C., Kappelle, L.J., Lo, R.H., van Dijk, E.J., de Vries, J., de Kort, P.L.M., van Rooij, W.J.J., van den Berg, J.S.P., van Hasselt, B.A.A.M., Aerden, L.A.M., Dallinga, R.J., Visser, M. C., Bot, J.C.J., Vroomen, P.C., Eshghi, O., Schreuder, T.H.C.M.L., Heijboer, R.J.J., Keizer, K., Tielbeek, A.V., den Hertog, H.M., Gerrits, D.G., van den Berg-Vos, R.M., Karas, G.B., Steyerberg, E.W., Flach, H.Z., Marquering, H.A., Sprengers, M.E.S., Jenniskens, S.F.M., Beenen, L.F.M., van den Berg, R., Koudstaal, P.J., van Zwam, W. H., Roos, Y.B.W.E.M., van der Lugt, A., van Oostenbrugge, R.J., Majoie, C.B.L.M., Dippel, D.W.J., 2015. A randomized trial of intraarterial treatment for acute ischemic stroke. N. Engl. J. Med. 372 (1), 11–20.

Campbell, B.C.V., Mitchell, P.J., Kleinig, T.J., Dewey, H.M., Churilov, L., Yassi, N., Yan, B., Dowling, R.J., Parsons, M.W., Oxley, T.J., Wu, T.Y., Brooks, M., Simpson, M. A., Miteff, F., Levi, C.R., Krause, M., Harrington, T.J., Faulder, K.C., Steinfort, B.S., Priglinger, M., Ang, T., Scroop, R., Barber, P.A., McGuinness, B., Wijeratne, T., Phan, T.G., Chong, W., Chandra, R.V., Bladin, C.F., Badve, M., Rice, H., de Villiers, L., Ma, H., Desmond, P.M., Donnan, G.A., Davis, S.M., 2015. Endovascular Therapy for Ischemic Stroke with Perfusion-Imaging Selection. N. Engl. J. Med. 372, 1009–1018. https://doi.org/10.1056/NEJMoa1414792.

Catanese, L., Tarsia, J., Fisher, M., 2017. Acute ischemic stroke therapy overview. Circ. Res. 120, 541–558. https://doi.org/10.1161/CIRCRESAHA.116.309278.

Coutts, S.B., Lev, M.H., Eliasziw, M., Roccatagliata, L., Hill, M.D., Schwamm, L.H., Pexman, J.H.W., Koroshetz, W.J., Hudon, M.E., Buchan, A.M., Gonzalez, R.G., Demchuk, A.M., 2004. ASPECTS on CTA Source Images Versus Unenhanced CT: Added Value in Predicting Final Infarct Extent and Clinical Outcome. Stroke 35, 2472–2476. https://doi.org/10.1161/01.STR.0000145330.14928.2a.

Fedorov, A., Beichel, R., Kalpathy-Cramer, J., Finet, J., Fillion-Robin, J.-C., Pujol, S., Bauer, C., Jennings, D., Fennessy, F., Sonka, M., Buatti, J., Aylward, S., Miller, J.V., Pieper, S., Kikinis, R., 2012. 3D slicer as an image computing platform for the quantitative imaging network. Magn. Reson. Imaging 30, 1323–1341. https://doi.org/10.1016/j.mri.2012.05.001.

Goyal, M., Menon, B.K., van Zwam, W.H., Dippel, D.W.J., Mitchell, P.J., Demchuk, A.M., Dávalos, A., Majoie, C.B.L.M., van der Lugt, A., de Miquel, M.A., Donnan, G.A., Roos, Y.B.W.E.M., Bonafe, A., Jahan, R., Diener, H.-C., van den Berg, L.A., Levy, E.I., Berkhemer, O.A., Pereira, V.M., Rempel, J., Millán, M., Davis, S.M., Roy, D., Thornton, J., Román, L.S., Ribó, M., Beumer, D., Stouch, B., Brown, S., Campbell, B. C.V., van Oostenbrugge, R.J., Saver, J.L., Hill, M.D., Jovin, T.G., 2016. Endovascular thrombectomy after large-vessel ischaemic stroke: a meta-analysis of individual patient data from five randomised trials. The Lancet 387, 1723–1731. https://doi.org/10.1016/S0140-6736(16)00163-X.

Hokkinen, L., Mäkelä, T., Savolainen, S., Kangasniemi, M., 2021. Evaluation of a CTA-based convolutional neural network for infarct volume prediction in anterior cerebral circulation ischaemic stroke. Eur. Radiol. Exp. 5, 25. https://doi.org/10.1186/s41747-021-00225-1.

Hornung, M., Taubmann, O., Ditt, H., Menze, B., Herman, P., Fransén, E., 2020. Detection of Ischemic Infarct Core in Non-contrast Computed Tomography, in: Liu, M., Yan, P., Lian, C., Cao, X. (Eds.), Machine Learning in Medical Imaging, Lecture Notes in Computer Science. Springer International Publishing, Cham, pp. 260–269. 10.1007/978-3-030-59861-7_27.

Jovin, T.G., Chamorro, A., Cobo, E., de Miquel, M.A., Molina, C.A., Rovira, A., San Román, L., Serena, J., Abilleira, S., Ribó, M., Millán, M., Urra, X., Cardona, P., López-Cancio, E., Tomasello, A., Castaño, C., Blasco, J., Aja, L., Dorado, L., Quesada, H., Rubiera, M., Hernandez-Pérez, M., Goyal, M., Demchuk, A.M., von Kummer, R., Gallofré, M., Dávalos, A., 2015. Thrombectomy within 8 Hours after Symptom Onset in Ischemic Stroke. N. Engl. J. Med. 372, 2296–2306. https://doi.org/10.1056/NEJMoa1503780.

Kim, Y., Lee, S., Abdelkhaleq, R., Lopez-Rivera, V., Navi, B., Kamel, H., Savitz, S.I., Czap, A.L., Grotta, J.C., McCullough, L.D., Krause, T.M., Giancardo, L., Vahidy, F.S., Sheth, S.A., 2021. Utilization and Availability of Advanced Imaging in Patients With

Acute Ischemic Stroke. Circulation: Cardiovascular Quality and Outcomes 14, e006989. https://doi.org/10.1161/CIRCOUTCOMES.120.006989.

Klein, S., Staring, M., Murphy, K., Viergever, M.A., Pluim, J.P.W., 2010. elastix: A Toolbox for Intensity-Based Medical Image Registration. IEEE Trans. Med. Imaging 29, 196–205. https://doi.org/10.1109/TMI.2009.2035616.

Krongold, M., Almekhlafi, M.A., Demchuk, A.M., Coutts, S.B., Frayne, R., Eilaghi, A., 2014. Final infarct volume estimation on 1-week follow-up MR imaging is feasible and is dependent on recanalization status. Neuroimage Clin 7, 1–6. https://doi.org/10.1016/j.nicl.2014.10.010.

Kuang, H., Menon, B.K., Sohn, S.I., Qiu, W., 2021. EIS-Net: Segmenting early infarct and scoring ASPECTS simultaneously on non-contrast CT of patients with acute ischemic stroke. Med. Image Anal. 70, 101984 https://doi.org/10.1016/j.media.2021.101984.

Lee, B.H., Hwang, Y.J., Kim, J.W., 2020. Delayed phase computed tomography angiography ASPECTS predicts clinical outcome and final infarct volume. PLOS ONE 15, e0239510. 10.1371/journal.pone.0239510.

Limaye, K., Bryant, A., Bathla, G., Dai, B., Kasab, S.A., Shaban, A., Samaniego, E.A., Hasan, D., Policeni, B., Leira, E., Derdeyn, C., Ortega-Gutierrez, S., 2019. Computed Tomography Angiogram Derived From Computed Tomography Perfusion Done with Low Iodine Volume Protocol Preserves Diagnostic Yield for Middle Cerebral Artery-M2 Occlusions. Journal of Stroke and Cerebrovascular Diseases 28, 104458. 10.1016/j.jstrokecerebrovasdis.2019.104458.

Lo, C.-M., Hung, P.-H., Hsieh, K.-L.-C., 2019. Computer-aided detection of hyperacute stroke based on relative radiomic patterns in computed tomography. Appl. Sci. 9, 1668. https://doi.org/10.3390/app9081668.

McDougall, C.C., Chan, L., Sachan, S., Guo, J., Sah, R.G., Menon, B.K., Demchuk, A.M., Hill, M.D., Forkert, N.D., d'Esterre, C.D., Barber, P.A., 2020. Dynamic CTA-Derived Perfusion Maps Predict Final Infarct Volume: The Simple Perfusion Reconstruction Algorithm. AJNR Am. J. Neuroradiol. 41, 2034–2040. https://doi.org/10.3174/ajnr.A6783.

Menon, B.K., d'Esterre, C.D., Qazi, E.M., Almekhlafi, M., Hahn, L., Demchuk, A.M., Goyal, M., 2015. Multiphase CT angiography: a new tool for the imaging triage of patients with acute ischemic stroke. Radiology 275, 510–520. https://doi.org/10.1148/radiol.15142256.

Peter, R., Korfiatis, P., Blezek, D., Beitia, A.O., Stepan-Buksakowska, I., Horinek, D., Flemming, K.D., Erickson, B.J., 2017. A quantitative symmetry-based analysis of hyperacute ischemic stroke lesions in non-contrast computed tomography. Med. Phys. 44, 192–199. https://doi.org/10.1002/mp.12015.

Qiu, W., Kuang, H., Teleg, E., Ospel, J.M., Sohn, S.I., Almekhlafi, M., Goyal, M., Hill, M. D., Demchuk, A.M., Menon, B.K., 2020. Machine learning for detecting early infarction in acute stroke with non–contrast-enhanced CT. Radiology 294, 638–644. https://doi.org/10.1148/radiol.2020191193.

Saver, J.L., Goyal, M., Bonafe, A., Diener, H.-C., Levy, E.I., Pereira, V.M., Albers, G.W., Cognard, C., Cohen, D.J., Hacke, W., Jansen, O., Jovin, T.G., Mattle, H.P., Nogueira, R.G., Siddiqui, A.H., Yavagal, D.R., Baxter, B.W., Devlin, T.G., Lopes, D.K., Reddy, V.K., du Mesnil de Rochemont, R., Singer, O.C., Jahan, R., 2015. Stent-Retriever Thrombectomy after Intravenous t-PA vs. t-PA Alone in Stroke. N. Engl. J. Med. 372 (24), 2285–2295.

Sheth, S.A., Lopez-Rivera, V., Barman, A., Grotta, J.C., Yoo, A.J., Lee, S., Inam, M.E., Savitz, S.I., Giancardo, L., 2019. Machine learning-enabled automated determination of acute ischemic core from computed tomography angiography. Stroke 50, 3093–3100. https://doi.org/10.1161/STROKEAHA.119.026189.

Srivatsan, A., Christensen, S., Lansberg, M.G., 2019. A relative noncontrast CT map to detect early ischemic changes in acute stroke. J. Neuroimaging 29, 182–186. https://doi.org/10.1111/jon.12593.

Virani, S.S., Alonso, A., Benjamin, E.J., Bittencourt, M.S., Callaway, C.W., Carson, A.P., Chamberlain, A.M., Chang, A.R., Cheng, S., Delling, F.N., Djousse, L., Elkind, M.S.V., Ferguson, J.F., Fornage, M., Khan, S.S., Kissela, B.M., Knutson, K.L., Kwan, T.W., Lackland, D.T., Lewis, T.T., Lichtman, J.H., Longenecker, C.T., Loop, M.S., Lutsey, P. L., Martin, S.S., Matsushita, K., Moran, A.E., Mussolino, M.E., Perak, A.M., Rosamond, W.D., Roth, G.A., Sampson, U.K.A., Satou, G.M., Schroeder, E.B., Shah, S. H., Shay, C.M., Spartano, N.L., Stokes, A., Tirschwell, D.L., VanWagner, L.B., Tsao, C. W., 2020. Heart disease and stroke statistics—2020 update: a report from the american heart association. Circulation 141 (9). https://doi.org/10.1161/CIR.0000000000000757.

Wu, G., Lin, J., Chen, X., Li, Z., Wang, Y., Zhao, J., Yu, J., 2019. Early identification of ischemic stroke in noncontrast computed tomography. Biomed. Signal Process. Control 52, 41–52. https://doi.org/10.1016/j.bspc.2019.03.008.

Zhang, R., Zhao, L., Lou, W., Abrigo, J.M., Mok, V.C.T., Chu, W.C.W., Wang, D., Shi, L., 2018. Automatic Segmentation of Acute Ischemic Stroke From DWI Using 3-D Fully Convolutional DenseNets. IEEE Trans. Med. Imaging 37, 2149–2160. https://doi.org/10.1109/TMI.2018.2821244.